Supporting Information

Photosensitizing metal-organic polyhedra combined with Co catalytic sites for CO_2 photoreduction

Jixin Li,[a‡*] Yaming Liu,[c‡] Kaiyue Ma,[b] Chunguang Li[b] and Zhan Shi[b*]

[a]School of Chemistry and Pharmaceutical Engineering, Jilin Institute of Chemical Technology, Jilin 132022, P. R. China.

[b]State Key Laboratory of Inorganic Synthesis and Preparative Chemistry, College of Chemistry, Jilin University, Changchun 130012, P. R. China.

[c]China Institute of Atomic Energy, Beijing 102413, P. R. China.

*E-mail: lijixin@jlict.edu.cn

*E-mail: zshi@mail.jlu.edu.cn

‡These authors contributed equally.

1. Reagents.

Acetonitrile (CH_3CN, Aladdin) and methanol (MeOH, Aladdin) used in the photocatalytic reaction were of GC grade. Triethanolamine (TEOA, ≥ 99%) was obtained from Adamas. 2, 2′-Bipyridine-5, 5′-dicarboxylic acid (BPYDC), $RuCl_3 \cdot 3H_2O$ and 2,2′-bipyridine (bpy) were obtained from Energy Chemical. BPYDC was recrystallized in DMF before use. Bis(cyclopentadienyl)zirconium dichloride ($ZrCp_2Cl_2$) was obtained from Sigma-Aldrich. LiCl was obtained from Alfa Aesar. $ZrCl_4$ was obtained from Acros. Other reagents were of analytical grade. All commercial chemicals were used without further purification unless otherwise mentioned.

2. Characterization.

Powder X-ray diffraction (PXRD) datas were collected on Bruker D8 Venture diffractometer using Cu Kα radiation source (λ = 1.54178 Å) with a scan speed of 1 °/min. Fourier Transform Infrared (FT-IR) spectra were measured with KBr pellets on a Bruker IFS-66 V/S FT-IR spectrometer. Inductively Coupled Plasma Optical Emission Spectrometer (ICP-OES) was conducted on Agilent 725. The method of dissolving MOPs and MOFs: 10 mg MOPs or MOFs and 5 mL nitric acid were put into a Teflon-lined stainless-steel autoclave and heated at 100 ℃ for 24 h. Scanning electron microscopy (SEM) was conducted using JEOL JSM-7800F. Transmission electron microscopy (TEM) was performed using FEI Tecnai G2 S-Twin with a field emission gun operated at 200 kV. Scanning transmission electron microscopy (STEM) and energy-dispersive X-ray spectroscopy (EDS) mapping were performed on JEM-2100F. X-ray photoelectron spectroscopy (XPS) data were collected on an ESCALAB250 spectrometer with an excitation source of Mg Kα radiation. Gas

sorption measurement was conducted using a Micromeritics ASAP 2020 system at desired temperatures. Before gas adsorption measurements, the samples were activated in vacuum at 150 ℃ for 12 h. Electrospray ionization mass spectrometry (ESI-MS) experiments were performed using a Thermo Fisher Scientific Q Exactive, and the test method refers to previous report[1]. ^{1}H-NMR spectra were collected on Bruker AVANCE III spectrometer at 600 MHz. Malverrn Panalytical Zetasizer Nano ZS90 was used to measure cage size. UV-visible absorption spectra were carried out through PerkinElmer Lambda 850. Steady-state photoluminescence (PL) emission spectra were recorded on an Edinburgh FLS920 fluorescence spectrometer in the air at room temperature.

3. Instruments and methods used in photocatalysis experiments.

The photocatalytic reaction was carried out in an all-glass automatic online trace gas analysis system (Labsolar-6A, Beijing Perfectlight). A 300 W Xe lamp (PLS-SXE300, Beijing Perfectlight) was employed as a light source, which was equipped with two cut filters to remove light with wavelengths less than 400 nm and longer than 780 nm. Light intensity was maintained at 400 mW/cm^2, which was detected by PL-MW2000 Photoradiometer (Beijing Perfectlight).

Gas products were analyzed by gas chromatography (GC, Shimadzu, GC-2014C ATF/SPL) with two flame ionization detectors (FID, one for detecting CO and CH_4, the other for detecting C_2H_6, C_2H_4 and C_2H_2) and a thermal conductivity detector (TCD, for detecting H_2). Gas products of the isotope tracer experiment were analyzed by gas chromatography-mass spectrometry (GC-MS, Agilent, 5977B GC/MSD).

4. Materials and methods.

Synthesis of $Ru(bpy)_2Cl_2$

$Ru(bpy)_2Cl_2$ was synthesized according to previous report[2]. $RuCl_3 \cdot 3H_2O$ (7.8 g), 2,2′-bipyridine (bpy, 9.36 g) and LiCl (8.4 g) were added to DMF (50 mL); then the mixture was refluxed for 9 h. After the solution was cooled to room temperature, acetone (250 mL) was poured into the solution and left overnight. The product was collected by filtration and washed with H_2O until the filtrate turned purple. Then the product was washed with ether three times and dried in vacuum to give a black solid.

Synthesis of $Ru(bpy)_2(bpydc)Cl_2$

$Ru(bpy)_2(bpydc)Cl_2$ (BPYDCRu) was synthesized according to previous report with modifications[3]. $Ru(bpy)_2Cl_2$ (800 mg) and BPYDC (505 mg) were added to EtOH/H_2O (V:V=1:1, 100 mL). The solution was refluxed for 48 h under Ar. After cooling to room temperature, the solution was filtrated and the filtrate was evaporated to complete dryness. The solid was redissolves in MeOH and filtered again. A large amount of THF was poured into the filtrate until the product was precipitated and left overnight. The product was collected by filtration and washed with THF. Then the red solid was dried in vacuum.

Synthesis of BPYDC-MOP

BPYDC-MOP was synthesized according to previous reports with modifications[4-6]. $ZrCp_2Cl_2$ (150 mg) and BPYDC (25 mg) were dispersed in DMF (5 mL). Then THF (2.5 mL) and H_2O (750 μL) were added to the solution. The mixture was heated at 65 °C for 8 h in a 20 mL Pyrex vial. After cooling to room temperature naturally, clear crystals were collected in a beaker and washed with a large amount of DMF until the solution becomes clear and transparent. The product was filtered and washed with THF three times. Then the white solid was dried in vacuum.

Synthesis of UiO-67-Ru

UiO-67-Ru was synthesized according to previous report with modifications[7]. BPYDCRu (29 mg), BPYDC (22 mg), acetic acid (300 μL) and H_2O (1 drop) were dispersed in DMF (6 mL). Then $ZrCl_4$ (30 mg) was added to the solution. The mixture was heated at 100 °C for 24 h in a 20 ml Pyrex vial. After cooling to room temperature naturally, orange solid was collected by filtration and washed with DMF until the filtrate becomes clear. Then the product was washed with MeOH three times and dried in vacuum.

Synthesis of UiO-67-Ru-Co

UiO-67-Ru (100 mg) was dispersed in MeOH (50 mL) by ultrasound and then $CoCl_2 \cdot 6H_2O$ (119 mg, 0.5 mmol) was added to it. The solution was stirred at room temperature for 24 h. The product was collected by filtration and washed with THF until the filtrate becomes colorless. The product was dried in air at room temperature for 24 h.

The ICP analysis results show that the content of Co element in UiO-67-Ru-Co is 1.02%, the content of Ru element is 3.81%, and the content of Zr element is 21.59%. The molecular formula of UiO-67-Ru-Co should be: $Zr_6O_4(OH)_4(C_{12}H_6N_2O_4)_{4.6}(C_{32}H_{22}N_6O_4Ru)_{0.96}(C_{12}H_6N_2O_4CoCl_2)_{0.44}(OAc)_{1.92}$. The content of Co element in UiO-67-Ru-Co is less than that in MOP-Ru-Co. This should be due to the limitation of the bulk structure of MOFs during the synthesis process.

5. Digestion of MOP

For the MOP that needs to be digested, 3 mg MOP was digested in 60 μL D_3PO_4. The solution was sonicated for 5 min and allowed to stand for 2 h, followed by the addition of 500 μL DMSO-d6 and 100 μL D_2O. Then, the mixture was analyzed by ^{1}H-NMR.

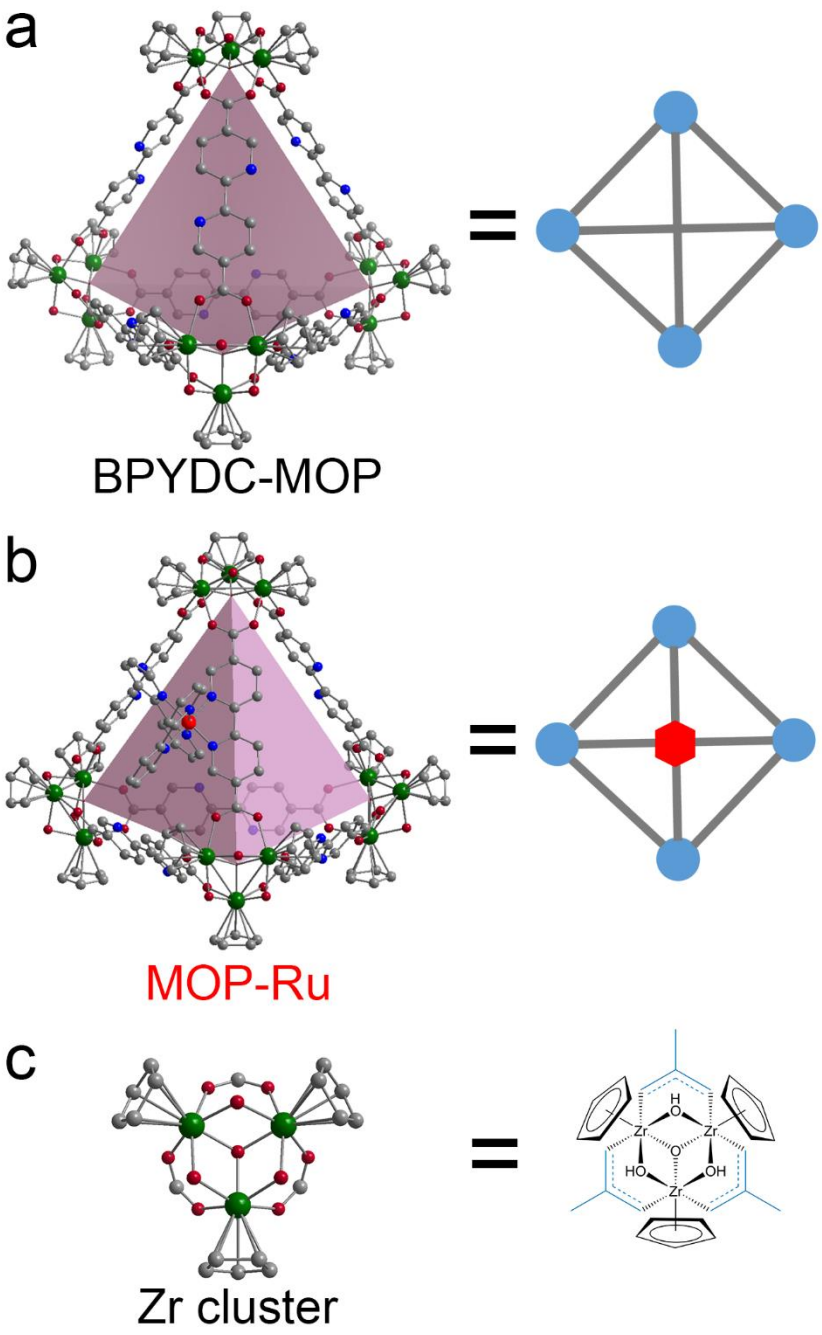

Figure S1. (a, b) Crystal structures and schematics of BPYDC-MOP and MOP-Ru. (c) Structure of Zr cluster. Zr, Ru, C, N and O atoms are shown in dark green, red, gray, blue and dark red, respectively.

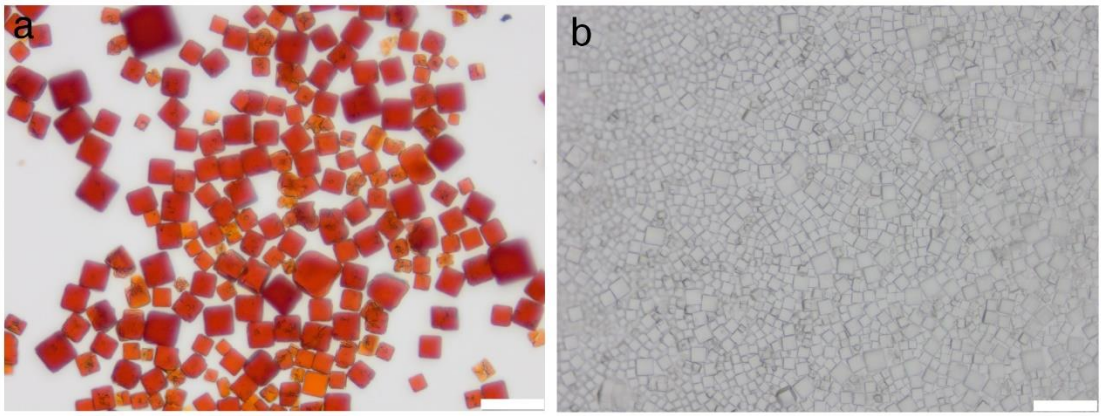

Figure S2. Optical photographs of (a) MOP-Ru and (b) BPYDC-MOP. Scale bar is 50 μm.

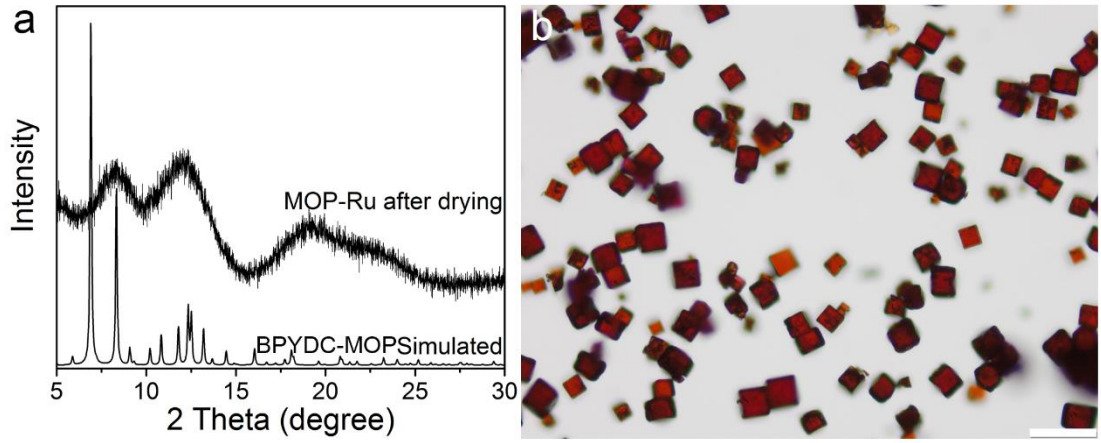

Figure S3. (a) PXRD patterns of MOP-Ru after drying and simulated BPYDC-MOP; and (b) Optical photograph of MOP-Ru after drying. Scale bar is 50 μm.

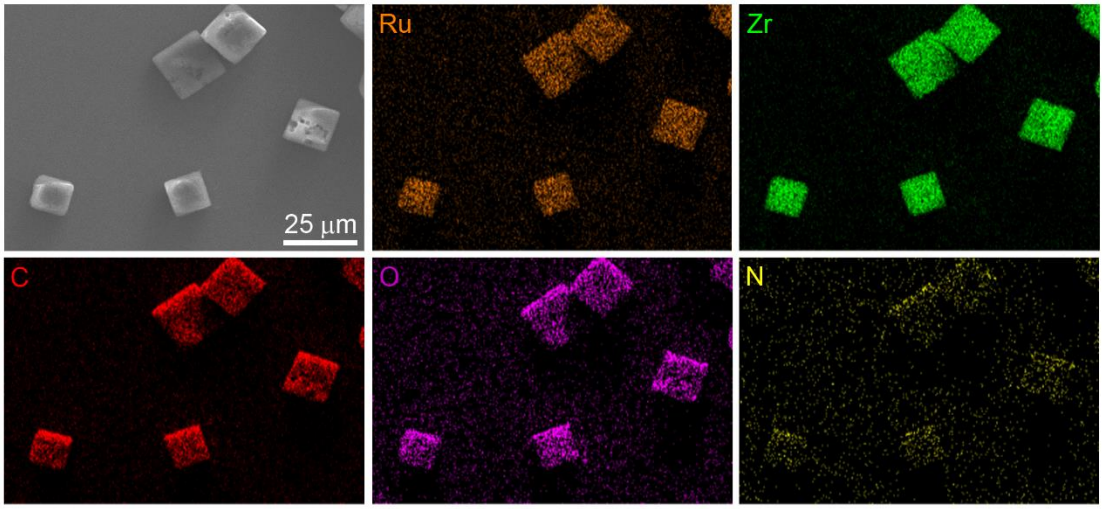

Figure S4. SEM and EDX elemental mapping images of MOP-Ru.

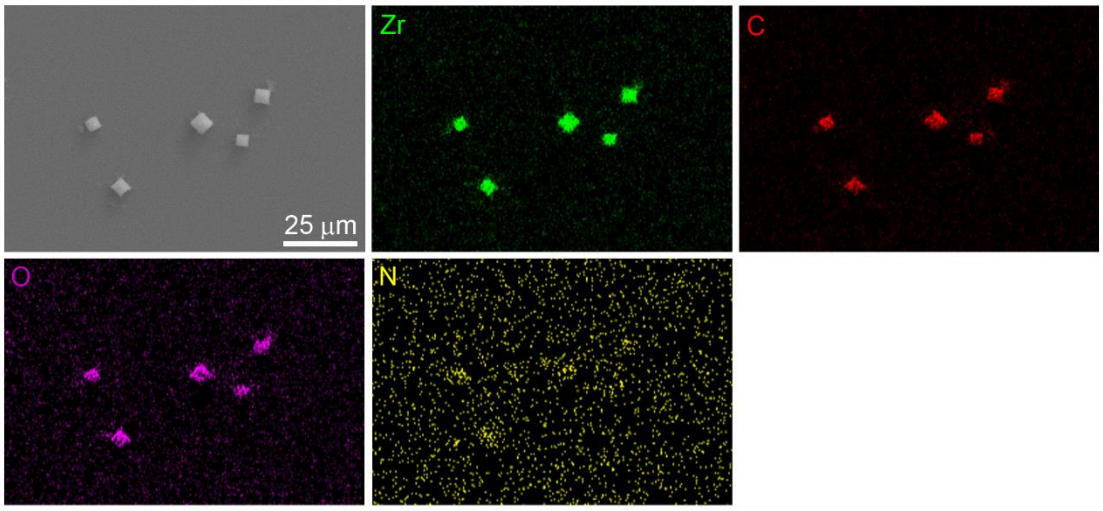

Figure S5. SEM and EDX elemental mapping images of BPYDC-MOP.

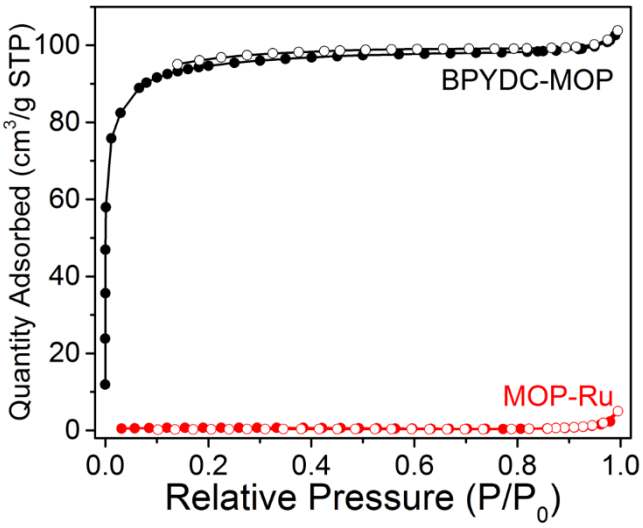

Figure S6. N_2 sorption isotherms of MOP-Ru and BPYDC-MOP at 77K.

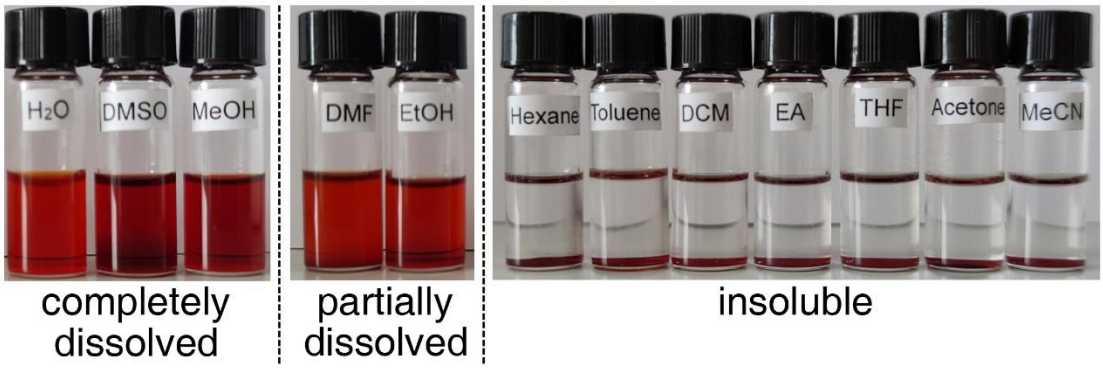

Figure S7. Solubility display of MOP-Ru in different solvents.

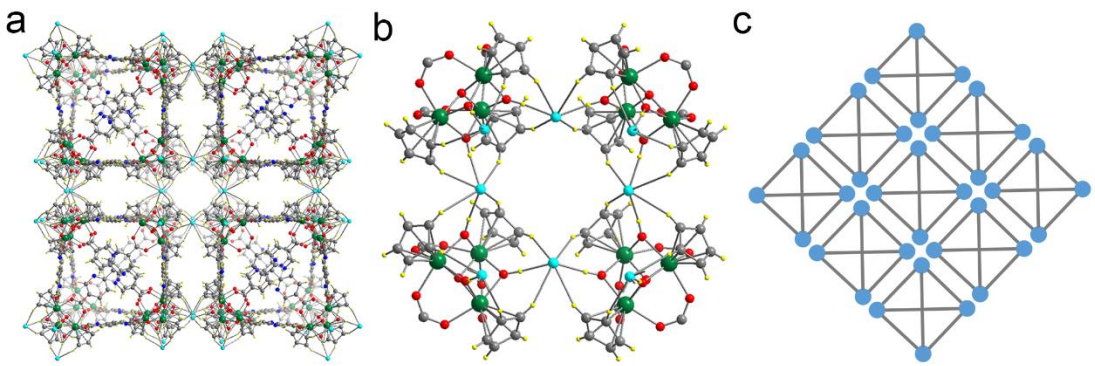

Figure S8. (a) The cages in BPYDC-MOP are linked together by ionic bonds to form a crystal; (b) A magnified view of the ionic bonds; Zr, Ru, C, N, O, H and Cl atoms are shown in dark green, red, gray, blue, dark red, yellow and bright blue respectively; and (c) schematics of many BPYDC-MOP cages aggregate into a crystal.

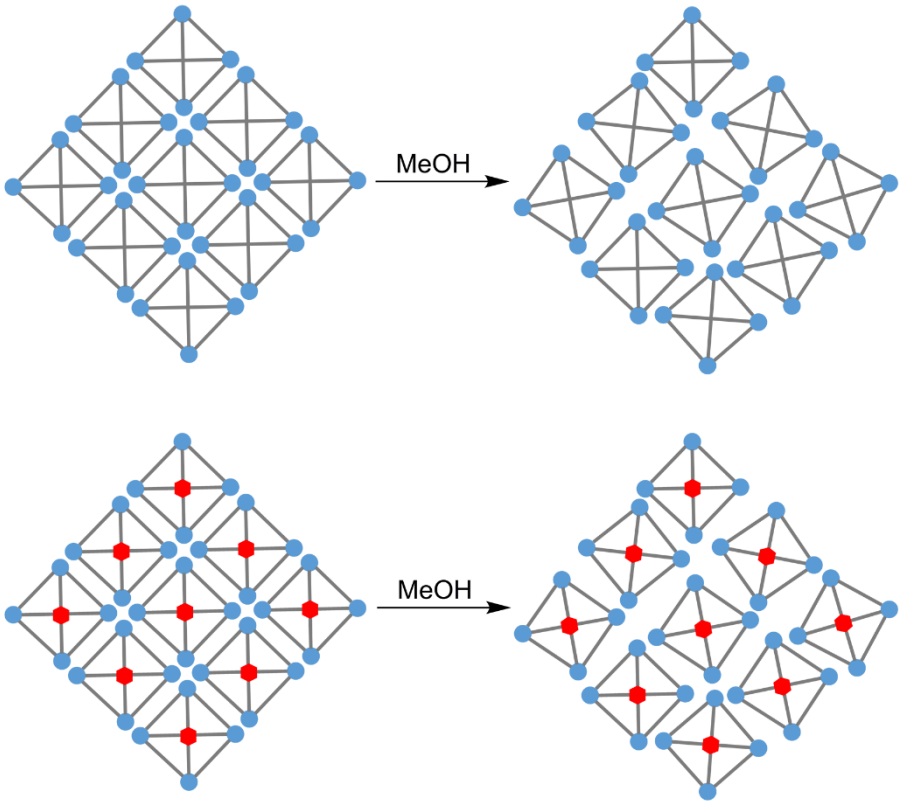

Figure S9. The regularly aggregated cages in BPYDC-MOP and MOP-Ru are dispersed into individual cages.

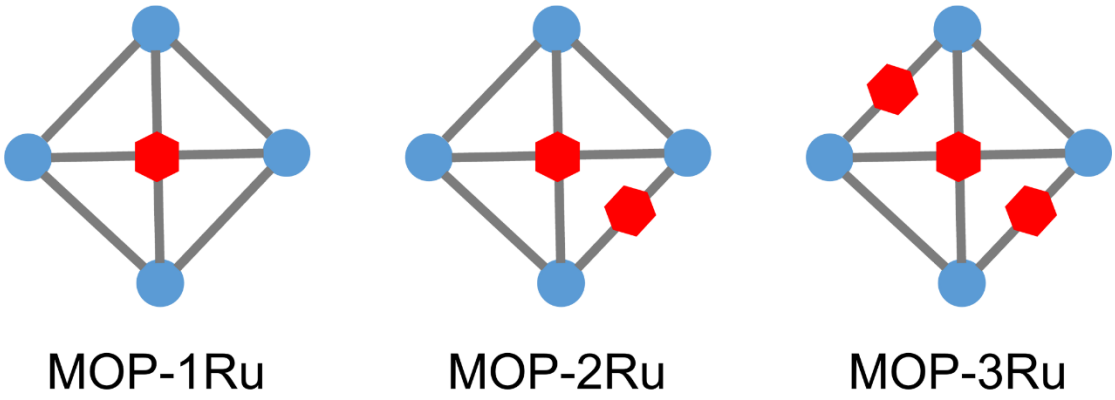

Figure S10. Schematics of MOP-Ru with different numbers of BPYDCRu ligands.

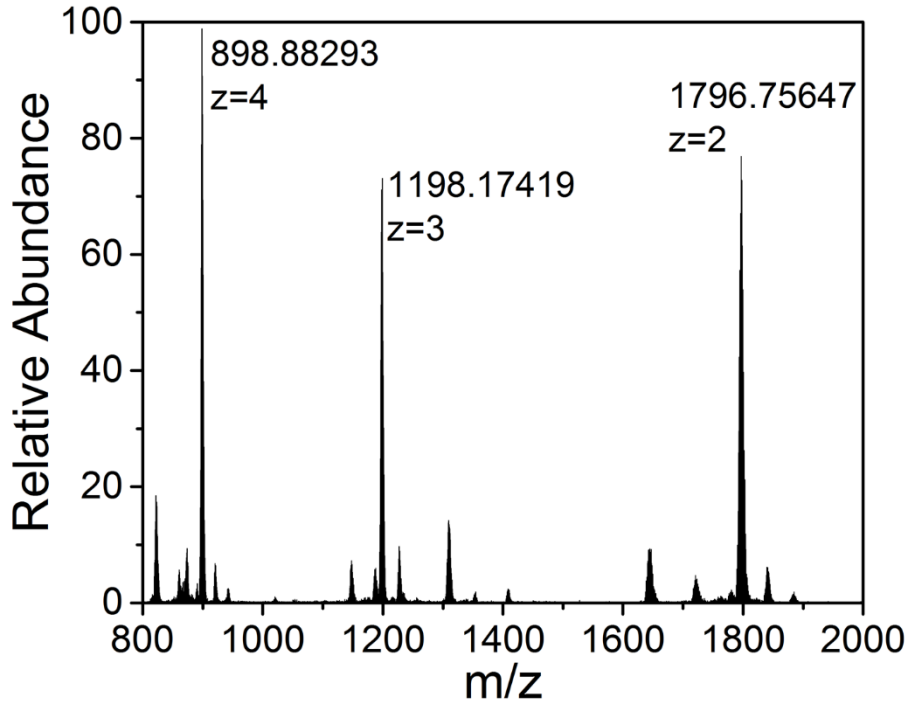

Figure S11. ESI mass spectrum of BPYDC-MOP. The three main peaks correspond to the BPYDC-MOP cages with 2, 3 and 4 charges respectively.

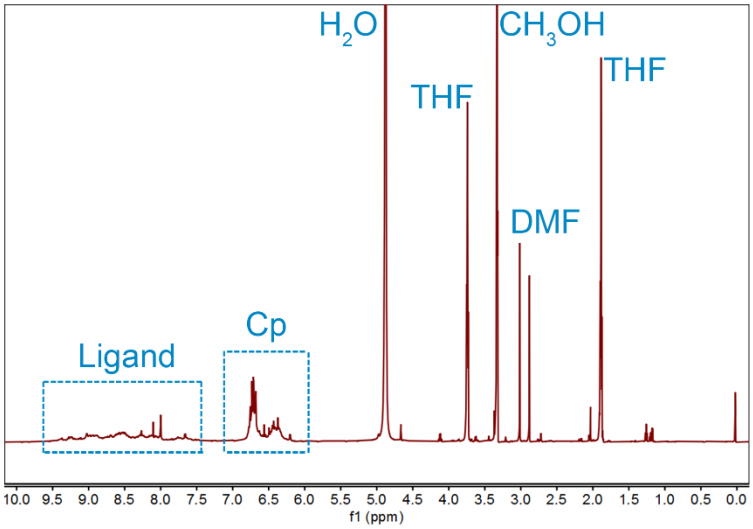

Figure S12. The complete ^{1}H-NMR spectrum of MOP-Ru.

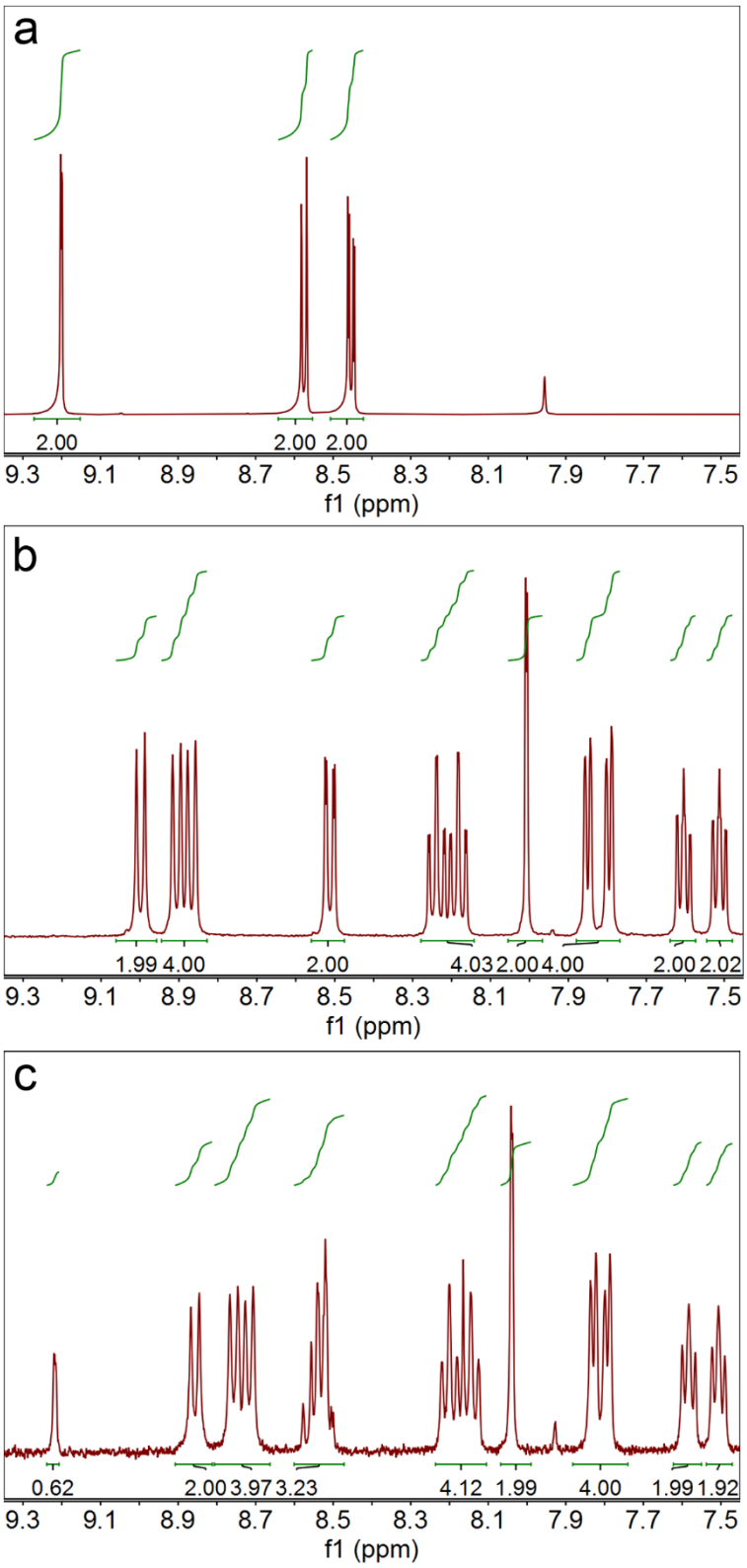

Figure S13. [1]H-NMR spectra of (a) BPYDC; (b) BPYDCRu; and (c) MOP-Ru after digestion.

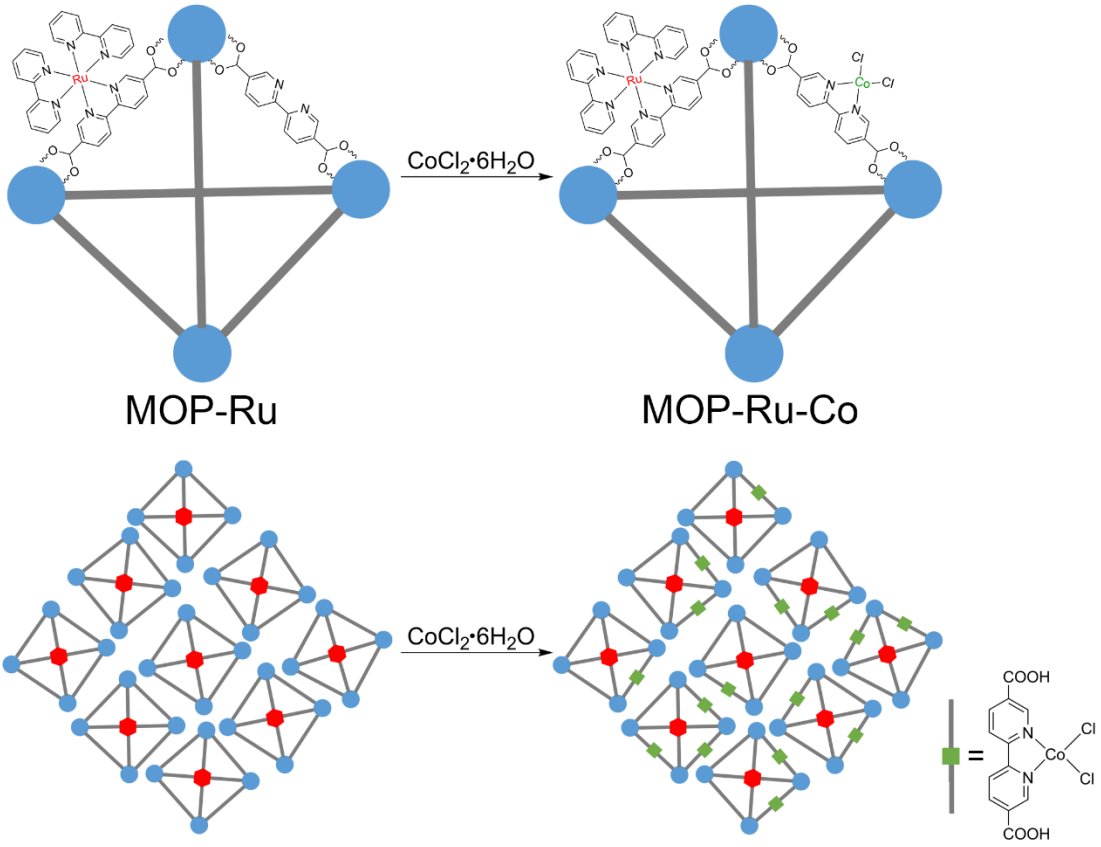

Figure S14. Schematics of synthesis MOP-Ru-Co.

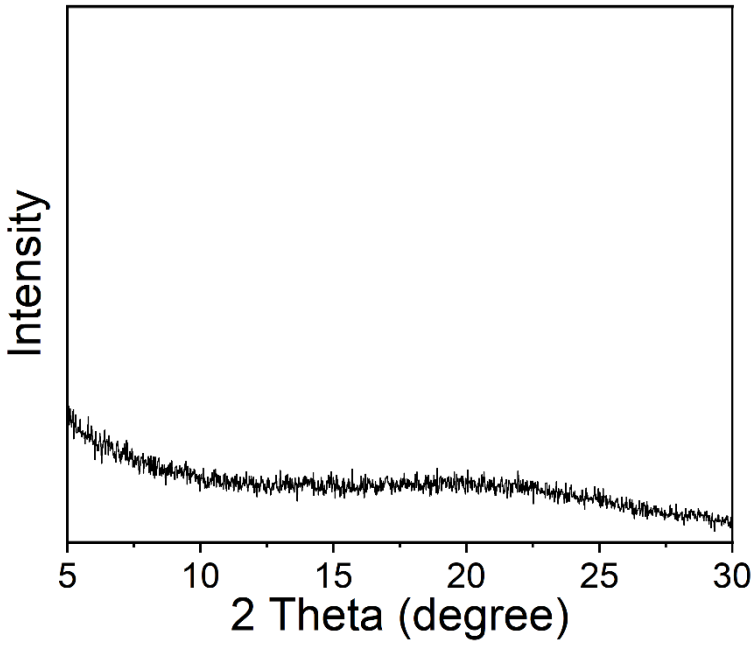

Figure S15. PXRD patterns of MOP-Ru-Co.

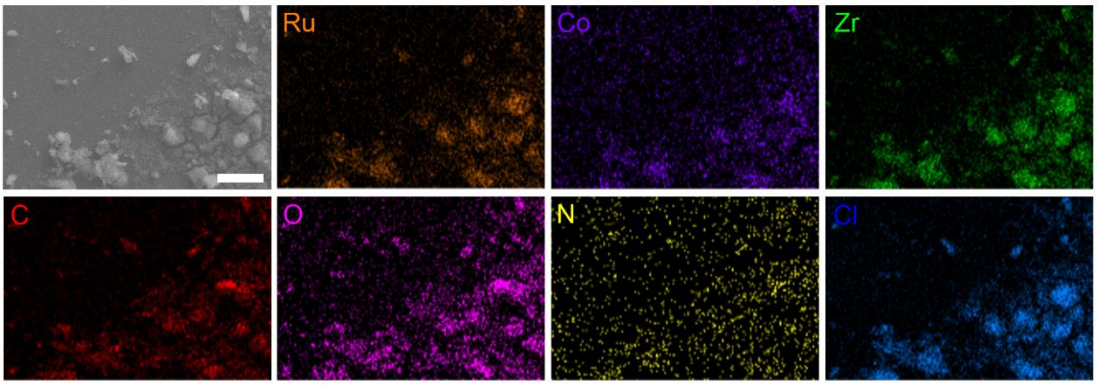

Figure S16. SEM and EDX elemental mapping images of MOP-Ru-Co.

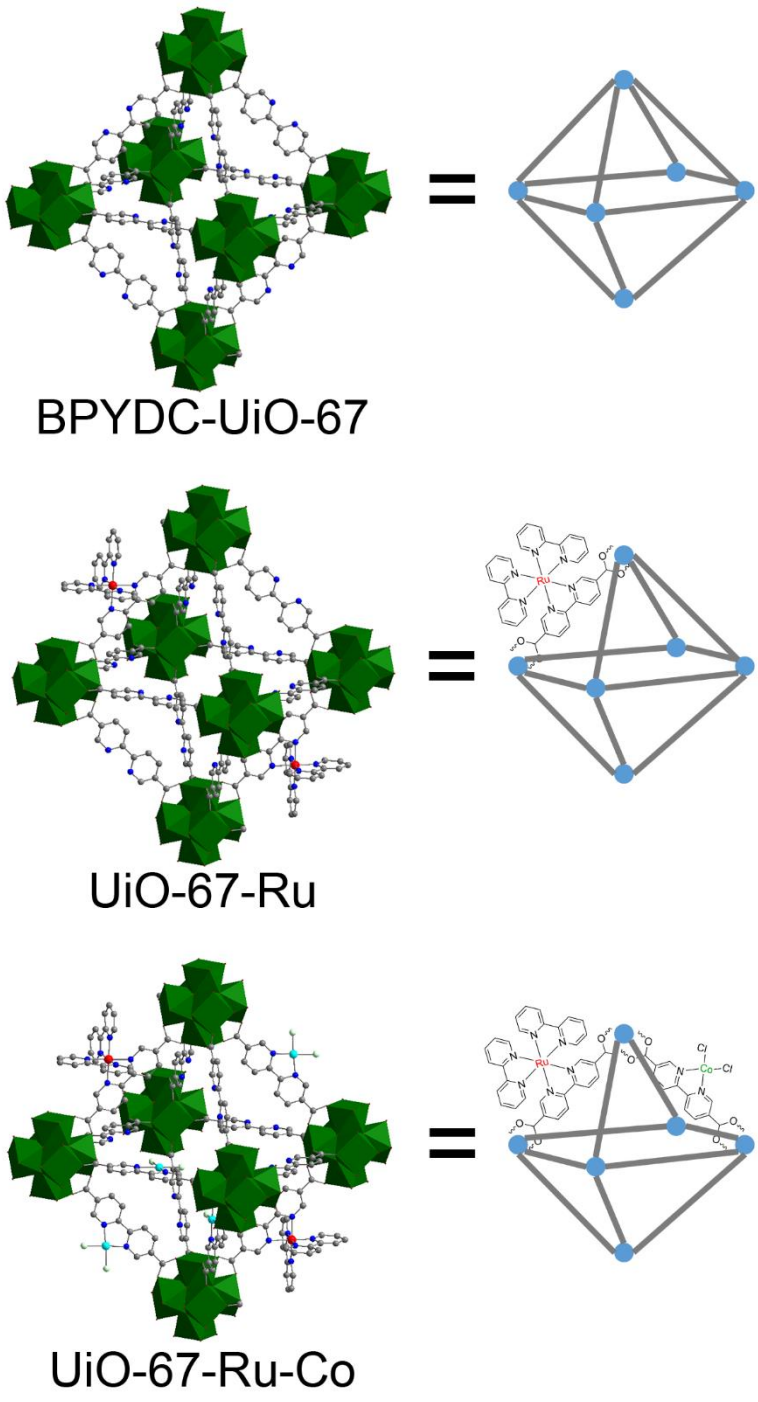

Figure S17. Crystal structures and schematics of BPYDC-UiO-67, UiO-67-Ru, and UiO-67-Ru-Co.

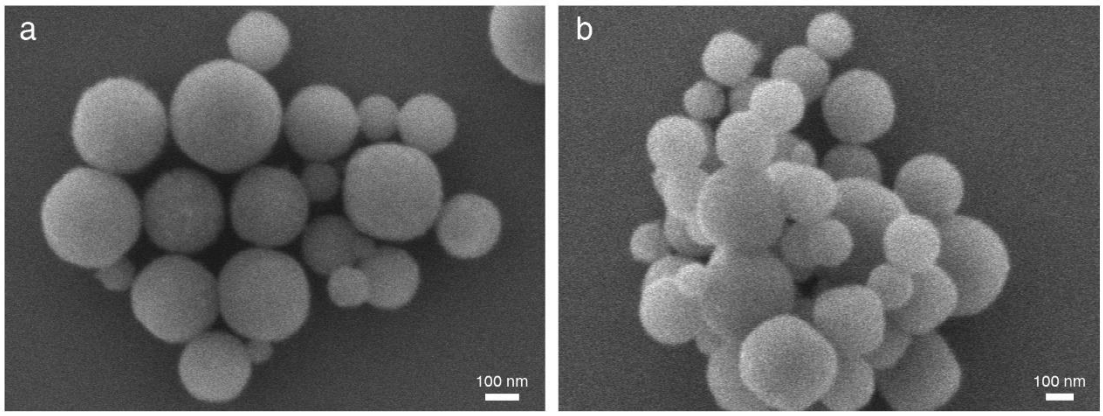

Figure S18. SEM images of (a)UiO-67-Ru and (b) UiO-67-Ru-Co.

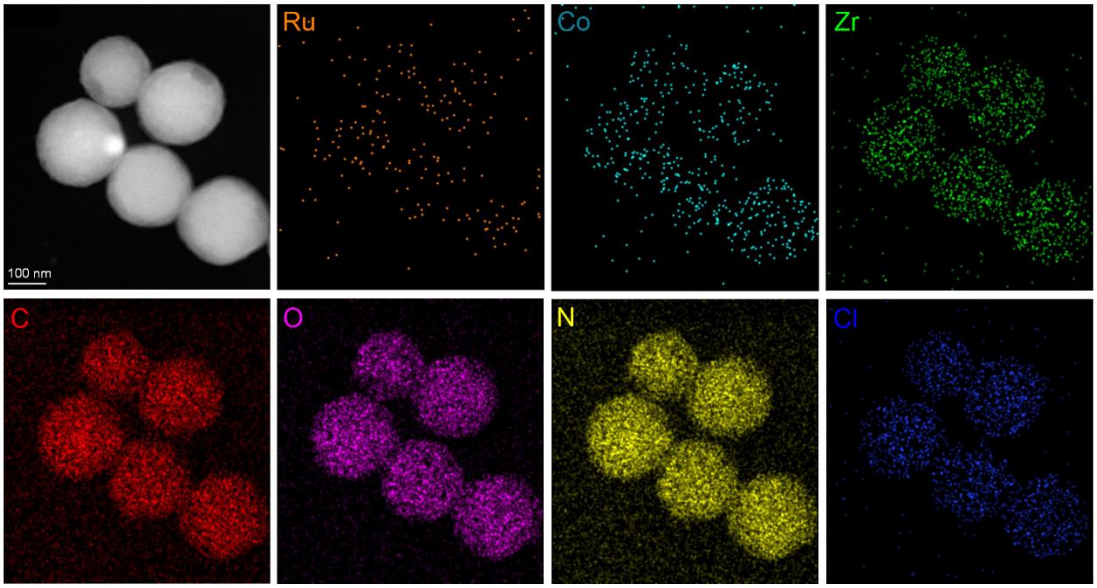

Figure S19. TEM-EDX elemental mapping images of UiO-67-Ru-Co.

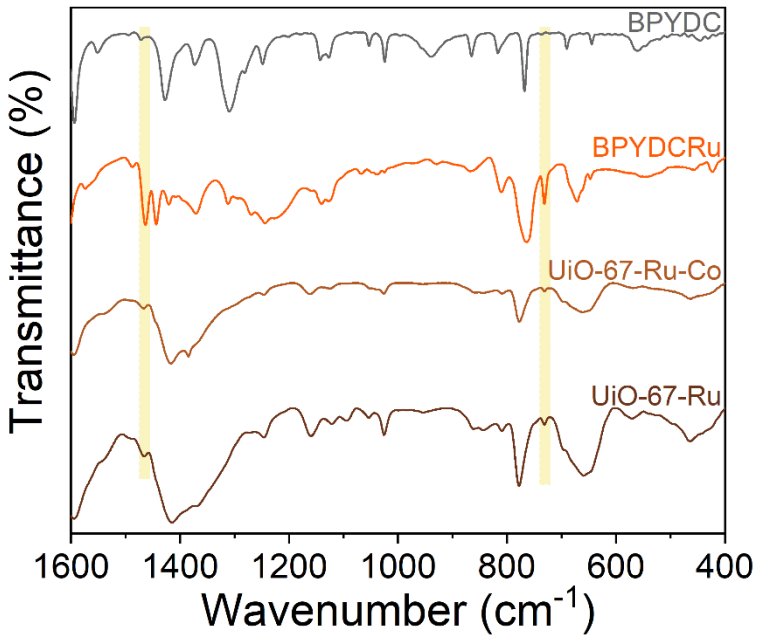

Figure S20. FT-IR spectra of UiO-67-Ru-Co, UiO-67-Ru, BPYDCRu and BPYDC.

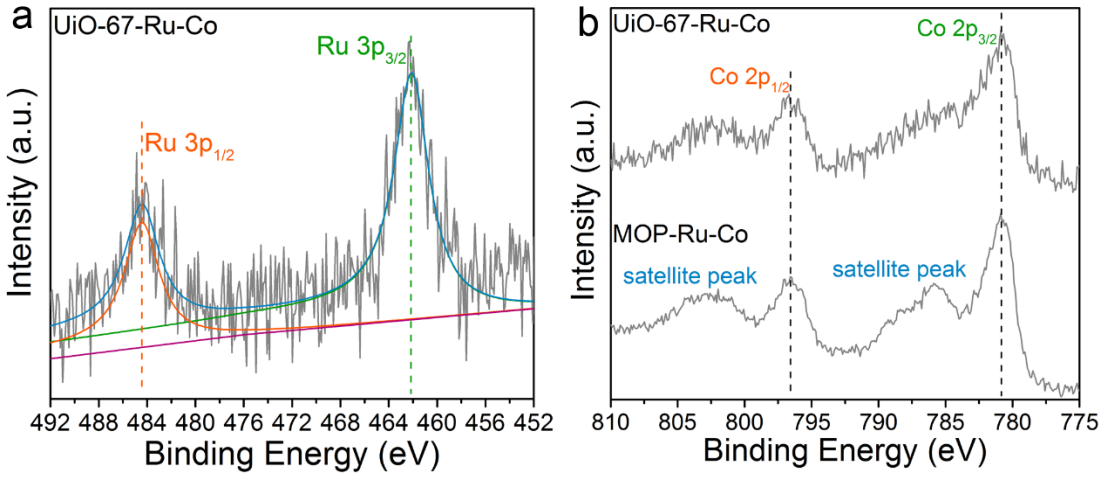

Figure S21. (a) XPS spectrum of Ru 3p in UiO-67-Ru-Co; and (b) XPS spectra of Co 2p in UiO-67-Ru-Co and MOP-Ru-Co.

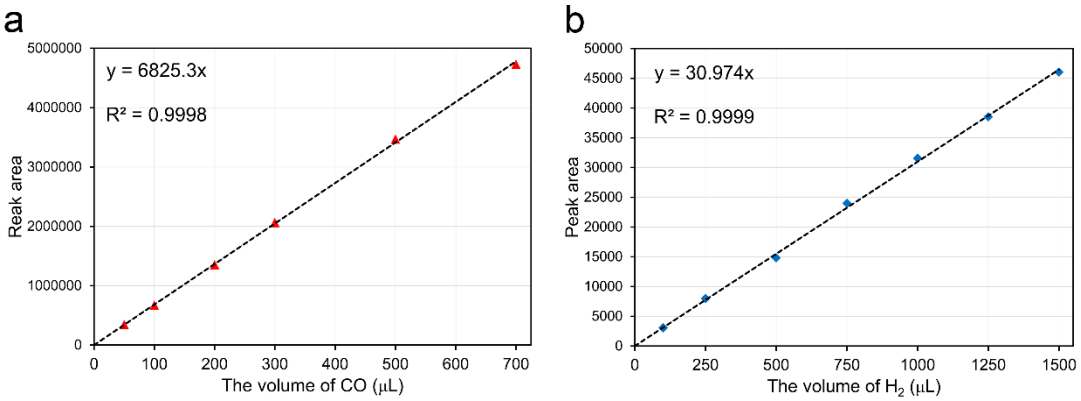

Figure S22. The calibration curves for CO and H_2.

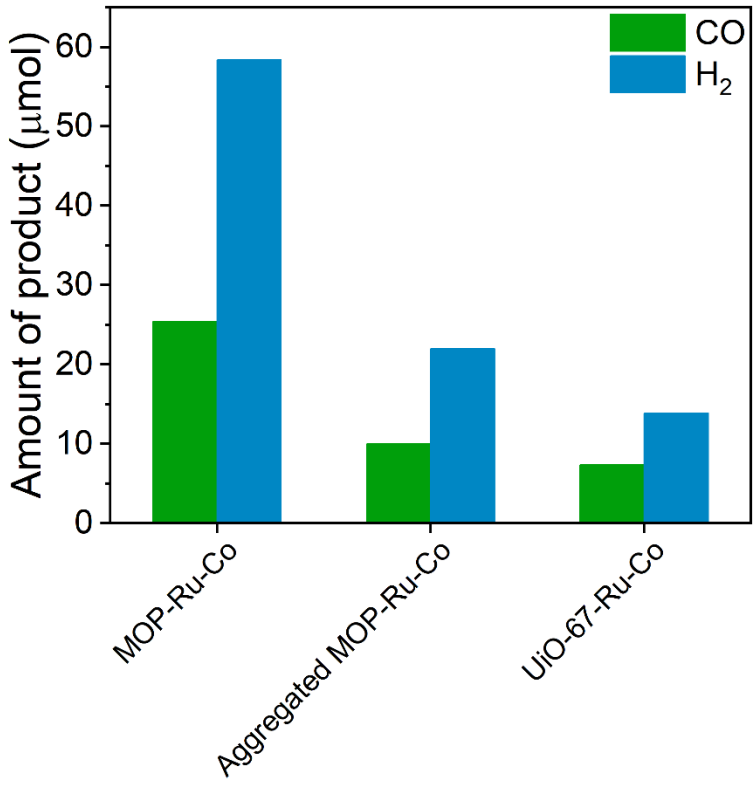

Figure S23. The amount of CO and H_2 produced by MOP-Ru-Co, Aggregated MOP-Ru-Co and UiO-67-Ru-Co after 6 h reaction.

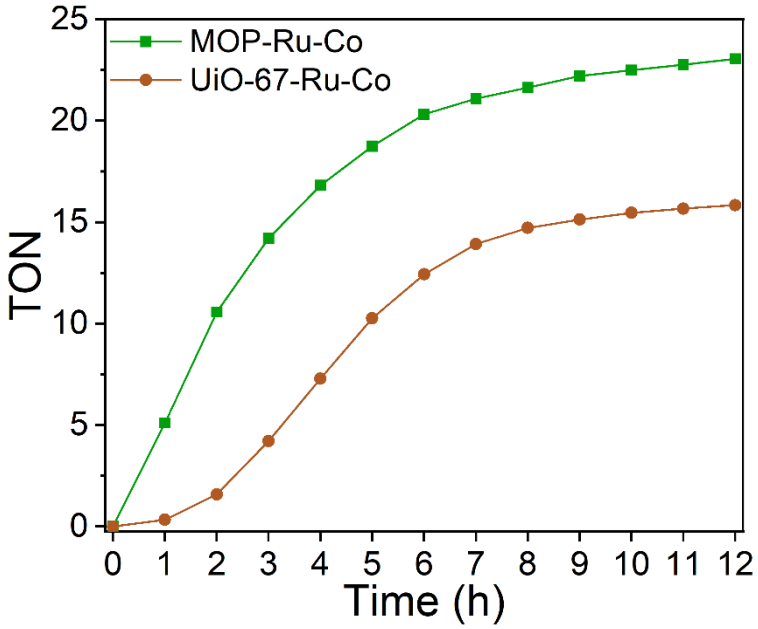

Figure S24. TON of MOP-Ru-Co and UiO-67-Ru-Co in the 12-hour experiment.

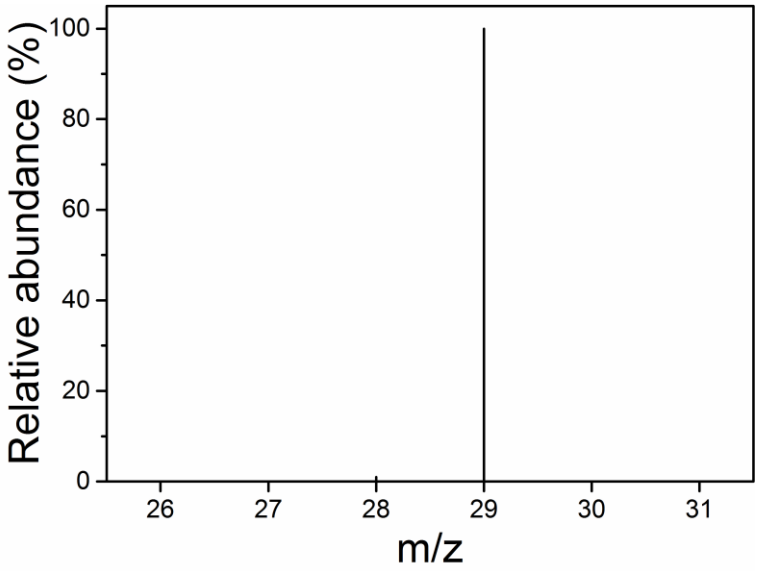

Figure S25. Mass spectrum of ^{29}CO obtained from the photocatalytic reaction.

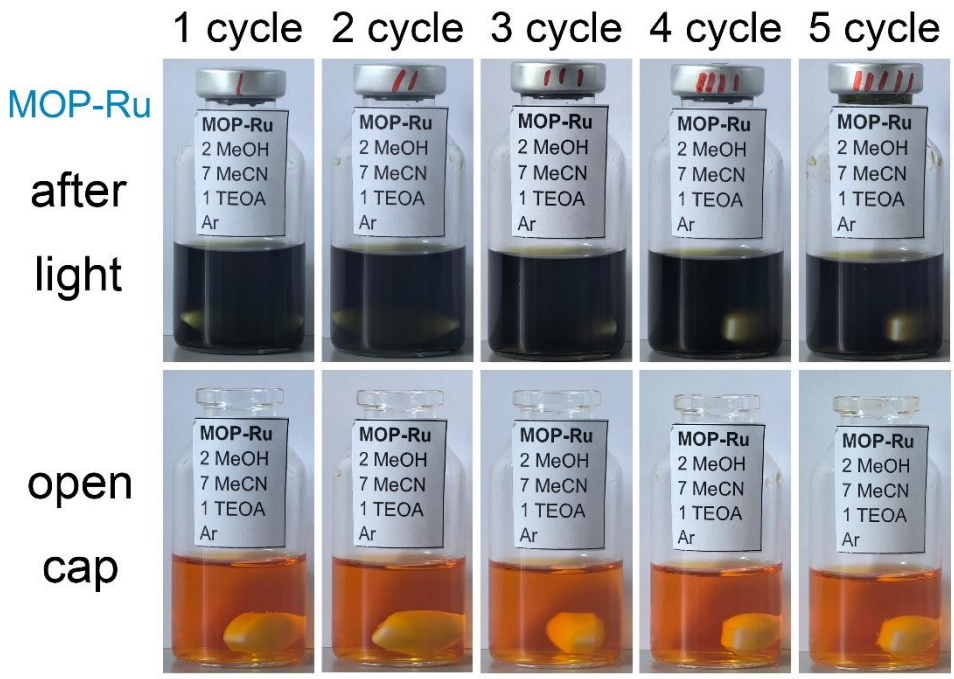

Figure S26. The cyclic test of the photochromic experiment of MOP-Ru.

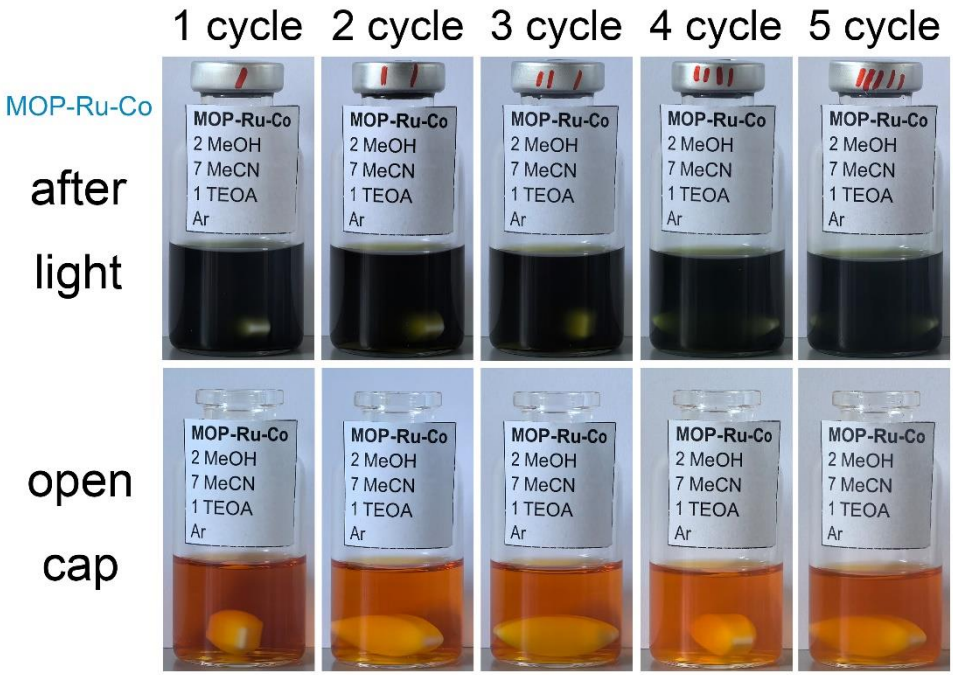

Figure S27. The cyclic test of the photochromic experiment of MOP-Ru-Co.

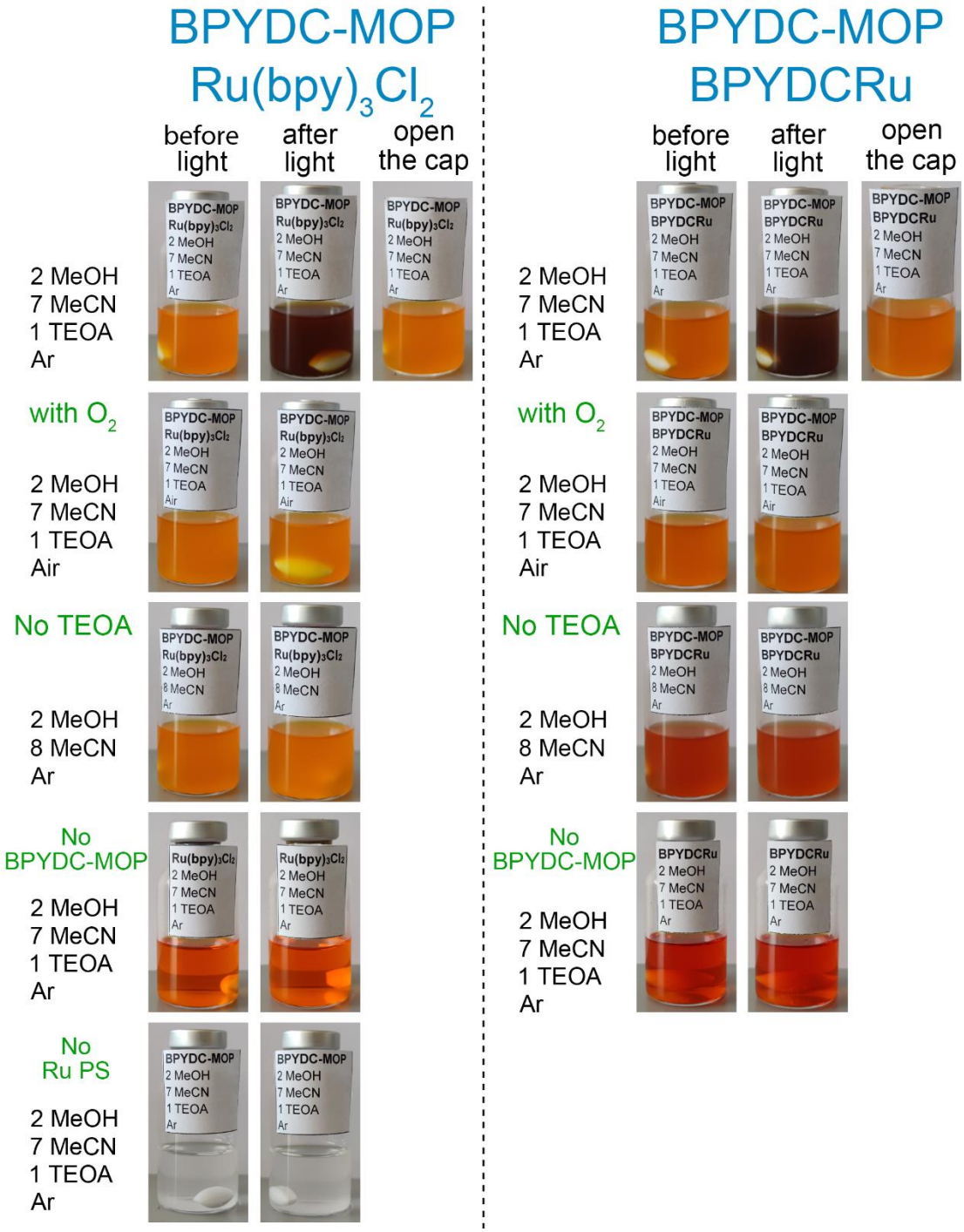

Figure S28. The photochromic phenomenon of $Ru(bpy)_3Cl_2$ and BPYDCRu combine with BPYDC-MOP in different experimental conditions.

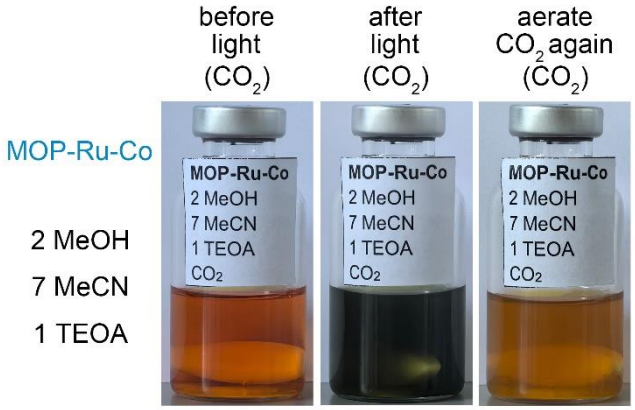

Figure S29. The photochromic phenomenon of MOP-Ru-Co under CO_2.

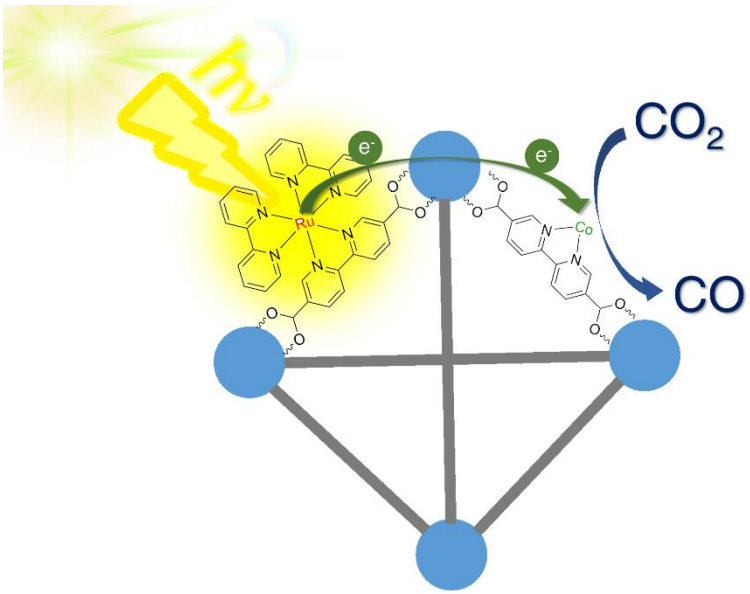

Figure S30. Proposed mechanism for visible light-driven CO_2 reduction catalyzed by MOP-Ru-Co.

.

Table S1. The changed reaction conditions in the control experiments.

Control experiments	Change of corresponding conditions
No Light	Wrap the reactor with aluminum foil
No Catalyst	No catalyst was added
No CO_2	Ar instead of CO_2 as reactant
No TEOA	10 mL MeOH and 40 mL MeCN as reaction solution

Table S2. The structures of MOP-Ru corresponding to the peaks appearing in the mass spectrum.

	Molecular formula	Molecular weight	2+	3+	4+	5+
1Ru	$C_{152}H_{124}O_{40}N_{16}Zr_{12}Ru$	4010.49	2003.25	1335.83	1002.12	
2Ru	$C_{172}H_{140}O_{40}N_{20}Zr_{12}Ru_2$	4423.94			1104.99	
2Ru-Cl	$C_{172}H_{140}O_{40}N_{20}Zr_{12}Ru_2Cl$	4459.39		1485.13	1114.10	
3Ru-Cl	$C_{192}H_{156}O_{40}N_{24}Zr_{12}Ru_3Cl$	4872.84				973.77
3Ru-2Cl	$C_{192}H_{156}O_{40}N_{24}Zr_{12}Ru_3Cl_2$	4908.29			1226.07	
3Ru-3Cl	$C_{192}H_{156}O_{40}N_{24}Zr_{12}Ru_3Cl_3$	4943.74		1646.58		

Note: There are three reasons for many peaks appear in the mass spectrum of MOP-Ru. Firstly, the active hydrogen of the hydroxyl group on the Zr cluster could be released into the solution as H^+, causing the MOP cage to lose a positive charge with each released H^+. Simultaneously, the BPYDCRu ligand contributed positive charges, and the precise counts of BPYDCRu ligands within each cage were undetermined. Additionally, MOP-Ru might have undergone electrostatic adsorption with Cl^-. Although there is so much uncertainty, one thing is certain, the peaks of MOP-Ru must have formed a group due to isotopic presence.

REFERENCE

1 Z. Xiao, H. F. Drake, Y. H. Rezenom, P. Cai and H.-C. Zhou, Structural Manipulation of a Zirconocene-Based Porous Coordination Cage Using External and Host-Guest Stimuli, *Small Struct.*, 2021, **3**, 2100133.

2 J. Li, X. Li, G. Xu, Z. Zheng, J. Deng and X. Ding, A self-deformable gel system with asymmetric shape change based on a gradient structure, *Chem. Commun.*, 2018, **54**, 11594-11597.

3 C. Wang, Z. Xie, K. E. deKrafft and W. Lin, Doping metal-organic frameworks for water oxidation, carbon dioxide reduction, and organic photocatalysis, *J. Am. Chem. Soc.*, 2011, **133**, 13445-13454.

4 C. Ji, W. Wang, E.-S. M. El-Sayed, G. Liu, Y. Si, K. Su, Z. Ju, F. Wu and D. Yuan, A high-efficiency dye-sensitized Pt(II) decorated metal-organic cage for visible-light-driven hydrogen production, *Appl. Catal. B-Environ.*, 2021, **285**, 119782.

5 S. Kim, S. Jee, K. M. Choi and D.-S. Shin, Single-atom Pd catalyst anchored on Zr-based metal-organic polyhedra for Suzuki-Miyaura cross coupling reactions in aqueous media, *Nano Res.*, 2020, **14**, 486-492.

6 G. Liu, Z. Ju, D. Yuan and M. Hong, In situ construction of a coordination zirconocene tetrahedron, *Inorg. Chem.*, 2013, **52**, 13815-13817.

7 M. Liu, Y.-F. Mu, S. Yao, S. Guo, X.-W. Guo, Z.-M. Zhang and T.-B. Lu, Photosensitizing single-site metal-organic framework enabling visible-light-driven CO_2 reduction for syngas production, *Appl. Catal. B-Environ.*, 2019, **245**, 496-501.